Proc. Natl. Acad. Sci. USA
Vol. 95, pp. 1601–1606, February 1998
Cell Biology

Opium alkaloid noscapine is an antitumor agent that arrests metaphase and induces apoptosis in dividing cells

KEQIANG YE*†, YONG KE‡, NAGALAKSHMI KESHAVA§, JOHN SHANKS†, JUDITH A. KAPP‡, RAJESHWAR R. TEKMAL§, JOHN PETROS¶, AND HARISH C. JOSHI*†‖

*Graduate Program in Biochemistry and Molecular Biology, Departments of †Anatomy and Cell Biology, ‡Pathology, §Gynecology–Obstetrics, and ¶Urology, Emory University School of Medicine, Atlanta, GA 30322

Edited by Thomas D. Pollard, Salk Institute for Biological Studies, La Jolla, CA, and approved December 17, 1997 (received for review July 17, 1997)

ABSTRACT **An alkaloid from opium, noscapine, is used as an antitussive drug and has low toxicity in humans and mice. We show that noscapine binds stoichiometrically to tubulin, alters its conformation, affects microtubule assembly, and arrests mammalian cells in mitosis. Furthermore, noscapine causes apoptosis in many cell types and has potent antitumor activity against solid murine lymphoid tumors (even when the drug was administered orally) and against human breast and bladder tumors implanted in nude mice. Because noscapine is water-soluble and absorbed after oral administration, its chemotherapeutic potential in human cancer merits thorough evaluation.**

Two important events in the cell division cycle are the duplication of the chromosomal DNA and the separation of the duplicated chromosomes. These events occur in two discrete phases: the synthetic phase (S phase) and the mitotic phase (M phase), which are separated from each other by G_1 and G_2 phases. The proper coordination of these events is achieved by checkpoint pathways that delay the progression of the cell cycle when proper completion of one phase is disrupted by physical damage or some other means (1, 2). Under normal circumstances, if the extent of damage is irreparable, most cells initiate a sequence of biochemical events leading to programmed cell death or apoptosis (for a recent review, see ref. 3). Deregulation in any one or more of these checkpoint mechanisms might lead to genetic instability, which is a primary step for a tumor to evolve into invasive malignant state. The chemotherapeutic management of various cancers is achieved by drugs that block S phase, M phase, or regulatory or metabolic pathways impinging on the cell cycle machinery. For example, some drugs affect the functions or structures of DNA or RNA; others interfere with enzymes involved in folate, purine, or pyrimidine metabolism or the function of mitotic spindles (4, 5). Antimitotic drugs such as vinca alkaloids and taxoids can arrest cells in M phase by interacting with the microtubules of the mitotic spindle.

It is now well accepted that dynamic assembly and disassembly of microtubules are required for the morphogenesis of mitotic spindle. This has lead to a tremendous interest in small organic molecules that modulate the dynamics of microtubules primarily because some of the microtubule interacting agents are useful for chemotherapeutic management of certain kinds of tumors. There are two classes of these antimicrotubule agents: those that prevent the assembly of tubulin and those that promote the assembly of tubulin. A prototypic example of a potent assembly inhibitor is colchicine. Others are analogs of colchicine, such as podophyllotoxin, MTC [2-methoxy-5-(2,3,4-trimethoxyphenyl)-2,4,6-cycloheptatrien-1-one], TCB (2,3,4-trimethoxy-4′-carbomethoxy-1,1′-biphenyl), and TKB (2,3,4-trimethoxy-4′-acetyl-1,1′-biphenyl), and vinca alkaloids. Taxol and its analogs represent the compounds that promote the assembly of microtubules. It is now clear that although all of these microtubule drugs prevent cell division, only a select few have been useful clinically. In addition, there are differences regarding the toxicity and the efficacy of these drugs for distinct classes of tumors (6).

Noscapine (Fig. 1), a phthalideisoquinoline alkaloid constituting 1–10% of the alkaloid content of opium, has been used as a cough suppressant in humans and in experimental animals (7–9). Mechanisms for its antitussive action are unknown, although animal studies have suggested central nervous system as a site of action. Karlsson *et al.* (10) and Mourey *et al.* (11) described high-affinity, saturable, and stereo-specific binding sites for noscapine in Guinea pig brain homogenates. In addition, noscapine has been shown to have low toxicity (7–9), although there are some reports of aneuploidy produced in cell cultures (12, 13). Additionally, noscapine has been used in humans orally, and the metabolic fate, bioavailability, and pharmacokinetics of noscapine by oral administration are relatively well studied (9, 14, 15). In oral administration of 50 mg, noscapine was rapidly absorbed and gave a maximum plasma concentration of 182 ng/ml after 1 h. From then on, the noscapine levels declined with a half-life of 124 min. The absolute oral bioavailability was 30% (8). The main metabolites of noscapine include cotarnine, hydrocotarnine, and meconine, which result from the cleavage of the C–C bond between isoquinoline and phthalide groups (14).

In this article, we show that the opium alkaloid noscapine shares chemical similarity with colchicine and podophyllotoxin, arrests cells at mitosis, and induces apoptosis. Furthermore, noscapine has also been shown to shrink murine thymoma and human breast and bladder tumors *in vivo*. In addition, we show that noscapine binds tubulin and alters microtubule assembly reactions *in vitro*.

MATERIALS AND METHODS

Noscapine. Noscapine (97% purity) was from Aldrich. The noscapine stock solution was prepared at 0.1 M in dimethyl sulfoxide (DMSO) and kept at −20°C.

Cells. HeLa cells were grown in DMEM (GIBCO/BRL) supplemented with 10% fetal calf serum, 1 mM L-glutamine, and 1% penicillin/streptomycin. The tumor cell line E.G7-OVA (H-2^b) (16) was grown in RPMI 1640 medium (GIBCO/BRL) with 10% fetal calf serum, 1 mM sodium pyruvate, 1 mM L-glutamine, 0.1% gentamycin, and 50 μM 2-mercaptoethanol. Cells were grown at 37°C in a 5% CO_2/95% air atmosphere.

The publication costs of this article were defrayed in part by page charge payment. This article must therefore be hereby marked "*advertisement*" in accordance with 18 U.S.C. §1734 solely to indicate this fact.

This paper was submitted directly (Track II) to the *Proceedings* office.
Abbreviations: DMSO, dimethyl sulfoxide; TUNEL, terminal deoxynucleotidyltransferase-mediated dUTP nick-end labeling.
‖To whom reprint requests should be addressed.

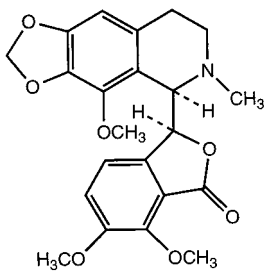

(*S, R*)-Noscapine

FIG. 1. Chemical structures of noscapine.

Cell viability was assessed by trypan blue exclusion analysis. Cell numbers were determined by using a hemacytometer (VWR Scientific).

Mice. Female C57BL/6 (H-2^b) mice, 8 to 12 weeks of age, were obtained from Harian–Sprague–Dawley. Mice were maintained on standard laboratory chow and water ad libitum in a temperature and light controlled environment.

Immunofluorescence of Microtubules. Cells in 10 ml of medium were incubated with 2 μl of DMSO or 20 μM noscapine (2 μl of a 0.1 M solution in DMSO), respectively. After 24 h, cells were fixed with cold (−20°C) methanol for 5 min and then rehydrated by PBS for 1 min. Nonspecific sites were blocked by incubating with 200 μl of 1% BSA in PBS at 37°C for 15 min. A mouse monoclonal antibody against α-tubulin (Amersham) was diluted 1:200 in PBS containing 1% BSA and incubated (200 μl) with the coverslips at 37°C for 1 h. Cells were then washed with 1% BSA/PBS for 10 min at room temperature before incubating with a 1:200 dilution of a rhodamine-labeled goat anti-mouse IgG antibody at room temperature for 45 min, and then the coverslips were rinsed with a 1% BSA/PBS solution for 10 min and incubated with 4,6-diamidino-2-phenylindole for another 10 min at room temperature. The coverslips containing the cells were then mounted with AquaMount (Lerner Laboratories, New Haven, CT) containing 0.01% 1,4-diazobicyclo(2,2,2)octane. Cells were examined with a Zeiss Axiovert 135 fluorescence microscope.

Flow Cytometric Analysis of Cell Cycle Status and Apoptosis. The flow cytometric evaluation of the cell cycle status was performed by a modification of a published method (17). Briefly, 2×10^6 untreated or noscapine-treated HeLa cells were centrifuged, washed twice with ice-cold PBS, and fixed in 70% ethanol. Tubes containing the cell pellets were stored at −20°C for at least 24 h. After this, the cells were centrifuged at 1,000 × *g* for 10 min and the supernatant was discarded. The pellets were resuspended in 30 μl of phosphate/citrate buffer (0.2 Na_2HPO_4/0.1 citric acid, pH 7.5) at room temperature for 30 min. Cells were then washed with 5 ml of PBS and incubated with propidium iodide (20 μg/ml)/RNase A (20 μg/ml) in PBS for 30 min. The samples were analyzed on a Coulter Elite flow cytometer.

DNA Fragmentation. Oligonucleosomal fragmentation of genomic DNA was determined as described (18). In brief, 3.3×10^6 cells in 10 ml of medium were incubated with 20 μM noscapine (2 μl of a 0.1 M solution in DMSO) for various times ranging from 0 to 24 h. At the end of incubation, cells were pelleted, washed twice with ice-cold PBS, and lysed on ice for 60 min in 250 μl of 1% Nonidet P-40/proteinase K (0.5 mg/ml) in PBS. Samples were centrifuged, the supernatants were removed and incubated with 5 μl of RNase A (10 mg/ml) at 37°C for 40 min, and 1 ml of anhydrous ethanol was added. Tubes were placed at −20°C for 20 min and then centrifuged to pellet DNA. After the samples were dry, the same amount DNA (10 μg) was electrophoresed at 80 V for 3 h through a 2% agarose gel containing ethidium bromide in TAE buffer (0.04 M Tris-acetate/0.001 M EDTA, pH 8.0). DNA bands were visualized under UV light. A 123-bp DNA ladder (GIBCO/BRL) was used as molecular size marker.

Cytochemical Staining of Apoptotic Cells. Morphological changes in the nuclear chromatin of cells undergoing apoptosis were detected by staining with 4′,6-diamidino-2-phenylindole (Boehringer Mannheim) as described (4). In brief, 0.5×10^6 to 3×10^6 cells were fixed with 4% glutaraldehyde/0.2% Triton X-100 in PBS, incubated at room temperature for 10 min, then centrifuged at 1,000 × *g* for 10 min, and resuspended in 20 μl of 0.1% 4,6-diamidino-2-phenylindole in ethanol. After a 15-min incubation at room temperature, 10 μl was placed on a glass slide, and 400 cells per slide were scored for the incidence of apoptotic chromatin changes with a Zeiss Axiovert model 135 fluorescence microscope.

Terminal Deoxynucleotidyltransferase-Mediated dUTP Nick-End Labeling (TUNEL) Assay for Apoptosis. The TUNEL assay was used as described (19). In brief, 2×10^6 cells in 10 ml of medium were incubated with 2 μl of 20 μM noscapine (2 μl of a 0.1 M solution in DMSO) for 24 h. Cells were pelleted and washed with ice-cold PBS twice, and lymphocytes were fixed in 4% paraformaldehyde in PBS and air-dried. The slides were rinsed with PBS and incubated with blocking solution (0.3% H_2O_2 in methanol) for 30 min at room temperature. The slides were rinsed with PBS again and incubated in permeability solution (0.1% Triton X-100/0.1% sodium citrate) on ice for 2 min. The slides were then washed twice with PBS, and 50 μl of TUNEL reaction mixture was added to samples on the slides and the slides were incubated in a humidified chamber for 60 min at 37°C. After the slides were rinsed with PBS, 50 μl of converter-POD solution (anti-fluorescein-POD, Fab fragment in 60 mM Tris-Hepes buffer/0.4% bovine immunoglobulin/0.2% Germall) was added on samples and incubated for 30 min at 37°C. The slides were rinsed with PBS three times, then 60 μl of 3,3′-diaminobenzidine solution was added on the samples, and the slides were incubated at room temperature for 10 min. After the slides were rinsed with PBS another three times, coverslips were mounted and analyzed with a Zeiss Axiovert light microscope. For the TUNEL staining of tissue sections, the paraffin-embedded tissues were dewaxed at 60°C for 15 min, then washed in xylene, and rehydrated through a graded series of ethanol and redistilled water. The resulting sections were incubated with proteinase K for 20 min at room temperature. The following steps were the same as above.

Noscapine Shrinks Murine Thymoma Solid Tumor. C57BL/6 mice were injected subcutaneously in the right flank with 2×10^6 E.G7-OVA cells. Three days later, mice were injected intraperitoneally or intragastrally every day for 3 weeks with 200 μl of saline ($n = 10$) or with 3 mg of noscapine dissolved in 200 μl of saline ($n = 10$). After 3 weeks, all mice were sacrificed by cervical dislocation. Tumors were removed and weighted. Tumor weights were individually plotted and comparisons between control and treatment groups were analyzed by the Student's *t* test. Statistical difference were considered significant if *P* values were less than 0.01.

Noscapine Eliminates Human Tumors. Three million human breast cancer cells (MCF-7, American Type Culture Collection) were injected in the axillary breast region of 12 female BALB/c athymic (nu/nu) nude mice 6–7 weeks of age (Harlan–Sprague). After the implanted mice grew tumors of 10–15 mm^3, 3 mg of noscapine dissolved in 0.2 ml of saline at pH 5.0 [120 mg/kg (body weight)] was administrated intraperitoneally to six mice for 3 weeks. The control mice received saline alone. The growth rate of tumors was monitored by measuring the diameters of the elliptical tumors in two perpendicular dimensions, and tumor volume was calculated by the formula: $4/3\pi r_1^2 r_2$ (r_1 and r_2 are the short and the long tumor radii, respectively). Mice were sacrificed after the

treatment, and the tumors were weighed, fixed, and processed for TUNEL staining to detect apoptosis.

Noscapine Binds Tubulins. Fluorescence titration for determining the binding constant was performed as described (20). In brief, at room temperature, 2 μM tubulin in 100 mM Pipes, pH 6.8/2 mM EGTA/1 mM $MgCl_2$ was excited at 278 nm, and the fluorescence emission spectra were recorded with bandwidths of 2 nm. The fluorescence emission intensity of noscapine at this excitation wavelength was negligible and at the concentration of noscapine used it gave no appreciable inner filter effect. The concentration of noscapine was raised in increments of 0.5 μM, until the decrease in the fluorescence intensity was saturated. The value of the dissociate constant and the number of sites were obtained from Scatchard plots by using the equation $r/[L]_{free} = n/K_d - r/K_d$, where r is the ratio of the concentration of bound ligand to the total protein concentration and n is the number of binding sites. CD spectra measurements were performed on Jasco 600 spectrometer, in cells with a 0.1-cm path at 25°C, as described (20).

Assays for Microtubule Assembly. The turbidity was recorded on spectrophotometer. The cuvettes (0.4-cm path) containing 100 mM Pipes, 2 mM EGTA, 1 mM $MgCl_2$, 1 mM GTP (PEM buffer, pH 6.8), and 20 μM noscapine in DMSO were kept at room temperature before the addition of 10 μM pure tubulin and shifting to 37°C. Tubulin and noscapine in PEM buffer did not show any detectable absorption at 350 nm. Noscapine was dissolved in DMSO at 0.8 mM and stocked at 4°C. The final concentration of DMSO was 4.5%. The cuvettes (1-cm path) contained PG buffer (10 mM sodium phosphate, 0.1 mM GTP, 1 mM EGTA, 16 mM $MgCl_2$, and 3.4 M glycerol at pH 7.0) and various concentrations of noscapine in DMSO. The assembly was monitored by measuring the changes in turbidity at 0.5-min intervals.

[^{3}H]Colchicine Binding Assays. The experimental procedures are as described with minor modification (21). Incubation of [^{3}H]colchicine (diluted to a final specific activity of 0.1 Ci/mmol; 1 Ci = 37 GBq) with 2 μM tubulin was carried out in PEM buffer (pH 6.8, 37°C) in the absence or presence of noscapine for 1.5 h. Bound colchicine was separated from free colchicine by gel filtration on column of Sephadex-25. [^{3}H]Colchicine in the effluent was then measured by liquid scintillation.

RESULTS

Discovery that Noscapine Arrests Cells at Mitosis. By scrutinizing the structures of known microtubule assembly inhibitors: colchicine, podophyllotoxin, MTC [2-methoxy-5-(2,3,4-trimethoxyphenyl)-2,4,6-cycloheptatrien-1-one], and some others, we noticed that many of these compounds contain a hydrophobic trimethoxyphenyl group; a variety of other hydrophobic domains such as lactone, tropolone, or other aromatic rings; and a small hydrophilic group such as OH and NH_2. To test whether other natural compounds might be useful antimitotic agents, we incubated HeLa cells with different concentrations of a series of natural compounds containing these shared structural features of antimitotic drugs. Fig. 2 shows the results from a 24-h treatment of human HeLa cells with 20 μM noscapine. In noscapine-treated cells, microtubule spindles, visualized by immunofluorescence staining of microtubules, look abnormal and fail to assemble chromosomes at the metaphase plate (Fig. 2*A*). Often we also observed multiple poles (Fig. 2*A*). Fig. 2*B* shows that noscapine-treated cells arrest with condensed chromosomes. Forty-eight hours after drug treatment, fewer cells were found arrested in mitosis and many cells showed large abnormal fragmented nuclei with apoptotic morphologies (see below). In addition to human HeLa cells, noscapine had this effect on a variety of cultured cell types.

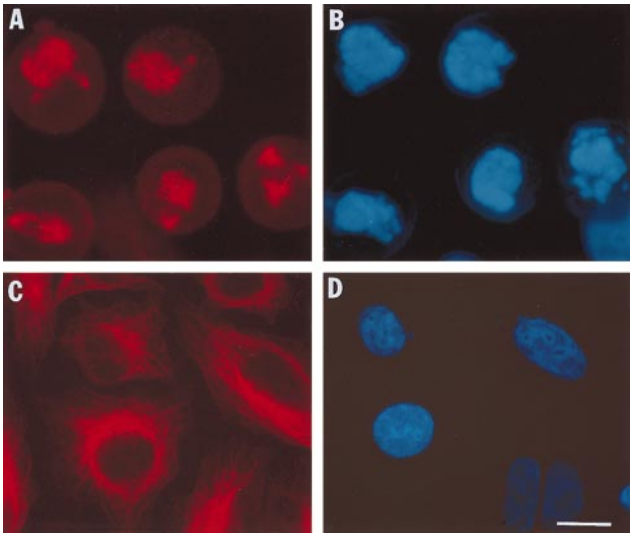

FIG. 2. Noscapine arrests HeLa cells at M phase. Immunofluorescent micrographs showing microtubule arrays (*A* and *C*) and DNA (*B* and *D*) in noscapine-treated HeLa cells (*A* and *B*) and control cells (*C* and *D*). (Bar = 15 μm.)

To quantify the effect of noscapine on the cell cycle, we performed fluorescence-activated cell sorting analysis of drug-treated or untreated HeLa cells at various times. As shown in Fig. 3*A*, the untreated cells exposed to the vehicle solvent (DMSO) showed normal cell cycle profile with 45.2% cells in G_1 phase, 12.9% cells in S phase, and 16.5% cells in G_2/M phase. However, After a 24-h noscapine treatment, the cells

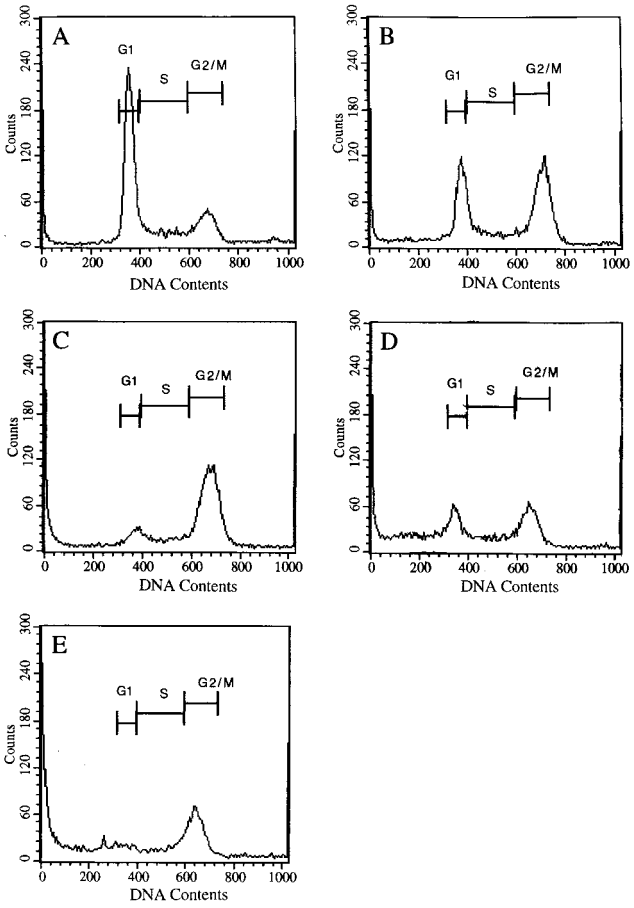

FIG. 3. Flow cytometric analysis of noscapine-treated HeLa cells at 0 (*A*), 12 (*B*), 24 (*C*), 36 (*D*), and 48 (*E*) h after noscapine treatment.

showed only 6.4% in G_1 phase, 11.1% in S phase, and 42.9% in G_2/M phase (Fig. 3*C*). As noscapine treatment time increased to 48 h, we found 5.2% cells in G*1* phase, 11.4% cells in S phase, and 22.3% cells in G_2/M phase. Additionally, more than 34% cells showed less than 2N DNA content, strongly suggesting DNA degradation, an event reminiscent of apoptosis (Fig. 3*E*).

Noscapine Induces Apoptosis in HeLa and Thymocyte Cells. Our ultimate aim was to test whether noscapine can be used to reduce tumor size in mice. We chose to test mouse thymocyte cell line E.G7-OVA, because these cells produce large palpable tumors within 3 weeks when injected subcutaneously in syngeneic mice. Like HeLa cells, these cells also arrested in mitosis and, on longer incubations, showed abnormal nuclear morphologies (see below).

To confirm whether the drug-treated cells went through the morphological and the biochemical stages characteristic of apoptosis, we performed immunofluorescence microscopy and DNA degradation analysis. As shown in Fig. 4*A*, DNA from the noscapine-treated E.G7-OVA cells displays a characteristic internucleosomal ladder of DNA fragments with an interval of ~200 bp. Such fragmentation appears within 8 h of drug application and increases with time (Fig. 4*A*). The number of noscapine-treated cells with apoptotic morphology increased dramatically and reached more than 50% in 24 h (Fig. 4*B*). Morphologically, the chromatin of noscapine-treated cells appeared in condensed spots reminiscent of apoptotic bodies (data not shown). We also used an alternative method for detecting DNA fragmentation *in situ*, the TUNEL assay (19). As shown in Fig. 4*D*, the apoptotic nuclei stain dark brown and are easily identifiable. Human HeLa cells yielded similar results (data not shown). We conclude that noscapine interferes with the mammalian cell cycle and induces cells to undergo apoptosis. Additionally, we also performed *in vitro* proliferation assays, the IC_{50} values for HeLa and thymocyte cells are 25 μM and 10 μM, respectively.

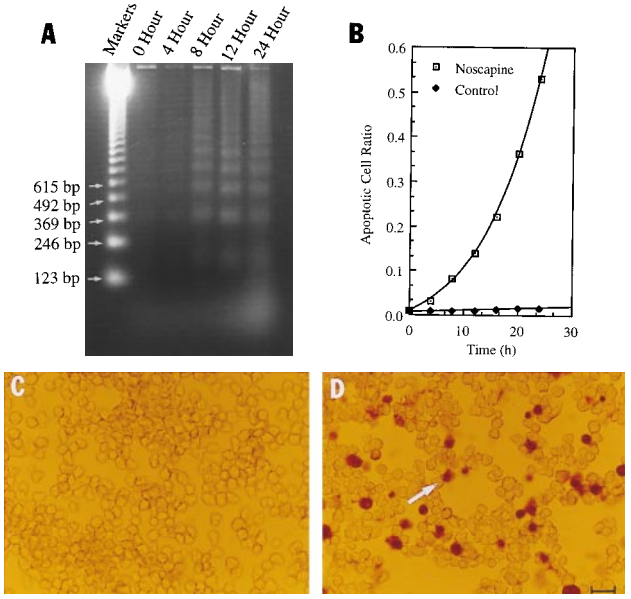

FIG. 4. Noscapine initiates apoptosis. (*A*) Progressive DNA degradation with increasing time of noscapine treatment. Lanes 2–6 contain 10 μg of DNA isolated from cells treated with 20 μM noscapine for 0 h, 4 h, 8 h, 12 h, and 24 h, respectively. Lane 1 contains molecular size markers. (*B*) Number of apoptotic cells with increasing time of incubation in 20 μM noscapine or the vehicle solution (DMSO). Cells with three or more visible chromatin masses were considered apoptotic. Each value represents the mean range of duplicate determinations of 400 cells. (*C* and *D*) Apoptotic cells revealed by using TUNEL assay. Apoptotic nuclei stained brown (arrowhead). (Bar = 30 μm.)

Noscapine Inhibits Growth of Murine and Human Tumors Implanted in Mice by Inducing Apoptosis. To examine whether noscapine could slow tumorgenesis *in vivo,* we injected female 8- to 12-week-old syngeneic (C57BL/6) mice subcutaneously with 2×10^6 E.G7-OVA thymoma cells. Three days later, one group of the mice were injected intraperitoneally or intragastrally with the 0.2 ml of vehicle saline solution (control), and another group received 0.2 ml of noscapine at 15 mg/ml [120 mg/kg (body weight)]. This dose was chosen on the basis of our *in vitro* proliferation assay and previous studies (22). These treatments were performed daily for 3 weeks. At this point, mice were sacrificed by cervical dislocation and photographed, and tumors were removed and weighed. The tumors were then fixed in 4% formaldehyde, dehydrated, and embedded in paraffin, and sections were cut and processed for histological analysis and for TUNEL staining to detect DNA fragmentation in apoptotic cells. Fig. 5 shows the weight (mean ± SEM) of control and experimental mice. It is clear from these data that noscapine reduces the tumor size quite dramatically. Additionally, there was not obvious weight loss or any other tissue toxicities detected after noscapine treatment.

To determine precisely the effect of noscapine on tumor growth, we examined the histological features of the cell injection site in tumor-cell-injected mice and tumor-cell-injected mice that were then treated with noscapine. In noscapine-treated mice, tumors were very small, and in some cases (6 of 10 mice) we could not detect any tumor. In the cases where we did find small tumor tissue, it was replete with holes. In control mice, the epidermis covers a very thin layer of dermis and a large (up to ~3 cm in diameter) lymphoid solid tumor containing packed thymoma cells (data not shown). By using the TUNEL assay, the treated tumors showed many cells with apoptotic morphologies that were stained darkly. The saline-treated control tumors showed only rare apoptotic cells and negligible TUNEL staining (data not shown). We conclude that, like in our *in vitro* studies, noscapine causes apoptosis in solid lymphoid tumors and possesses a potent antitumor activity *in vivo*.

To test whether noscapine can inhibit growth of human breast and bladder cancer cells, we did the *in vitro* proliferation assays, the IC_{50} values for MCF-7 and Renal 1983 cell lines were 42.3 μM and 39.1 μM, respectively. To test whether noscapine can also inhibit growth of human tumors *in vivo*, we implanted 3×10^6 MCF-7 human breast cancer cells at two axillary sites in 12 female athymic nude mice. After establishment of tumors (10–15 mm^3), six mice were given intraperitoneally 3 mg of noscapine [120 mg/kg (body weight)] per day for 3 weeks. As shown in Fig. 6*B*, human breast tumors regressed by 80% at the end of a 3-week treatment. TUNEL assay of the treated tumor sections (Fig. 6*D*) showed increased

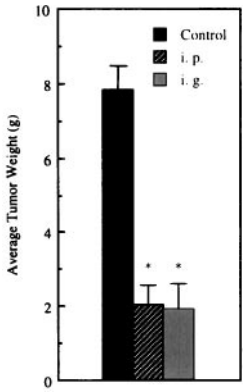

FIG. 5. Inhibition of tumor growth with noscapine. Tumor weights from each group were averaged and compared with the control group. *, Results are significantly different when compared with control group ($P < 0.01$).

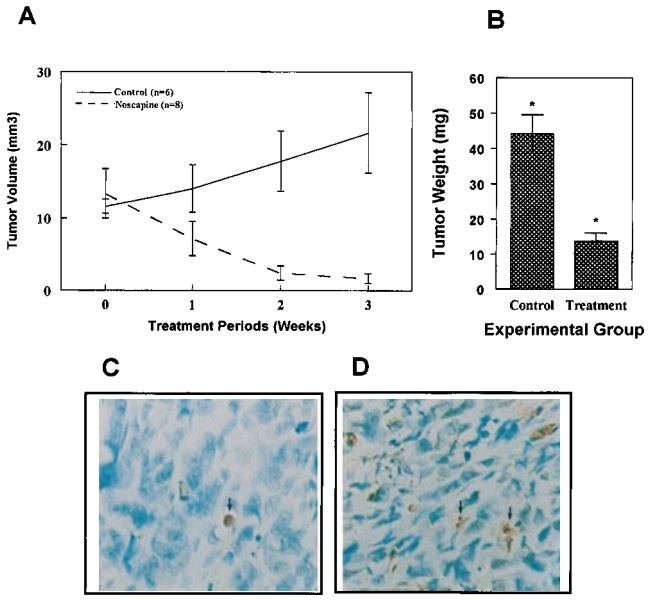

FIG. 6. Effect of noscapine on human breast tumor growth. (*A*) Reduction of tumor volume during the treatment period. (*B*) The average tumor weight. (*C* and *D*) Apoptotic cells (arrows) in untreated control and noscapine-treated cells, respectively. (Bar = 35 μm.)

apoptotic activity when compared with control untreated tumors (Fig. 6*C*). In addition, in a similar treatment regime, we also measured more than 60% reduction of a human transitional cell carcinoma implanted in athymic mice (data not shown). We conclude that noscapine may have activity against a wide variety of human tumors.

Noscapine Binding Induces a Conformational Change in Tubulin and Alters Microtubule Assembly. To test whether noscapine interacts directly with tubulin, we examined tubulin fluorescence in the presence or absence of noscapine. The characteristic tubulin fluorescence emission spectrum was quenched by noscapine in a concentration-dependent manner (Fig. 7*A*), and this effect was saturable (Fig. 7*B Inset*). Noscapine itself produced negligible fluorescent signal when excited at 278 nm (data not shown). Because radiolabeled noscapine is not currently available, we assumed one noscapine binding site per tubulin dimer for Scatchard plot analysis. The values of the dissociation constant and the number of noscapine binding sites on tubulin were obtained according to the formula: $r/[L]_{free} = n/K_d - r/K_d$, where r is the ratio of the concentration of bound ligand to the total protein concentration and n represents the maximum number of binding sites. This analysis gave an apparent dissociation constant K_d of $1.86 \pm 0.34 \times 10^{-6}$ M and an stoichiometry of 0.95 ± 0.02 noscapine molecule per tubulin subunit (Fig. 7*B*), but we still cannot exclude the possibility of two equal affinity binding sites on tubulin.

These fluorescence quenching studies indicated that noscapine might induce some conformational changes upon binding tubulin. To further evaluate the extent of conformational changes in tubulin upon binding noscapine, we examined the CD spectrum of tubulin in the absence and in the presence of noscapine. Fig. 7*C* shows that noscapine caused a molar ellipticity increment of $-2 \times 10^3 \pm 500$ degrees·cm^2/dmol at 217 nm, consistent with noscapine-induced structural perturbation in tubulin.

Noscapine shares some chemical similarity with podophyllotoxin and colchicine. To test whether noscapine and colchicine bind to the same site, we performed a [^{3}H]colchicine competition experiment with noscapine (Fig. 7*D*). The results show that noscapine is unable to compete with colchicine binding, probably suggesting that noscapine binds to a site other than the colchicine binding site. We also tested whether noscapine competes with colchicine for binding tubulin by determining the fluorescence

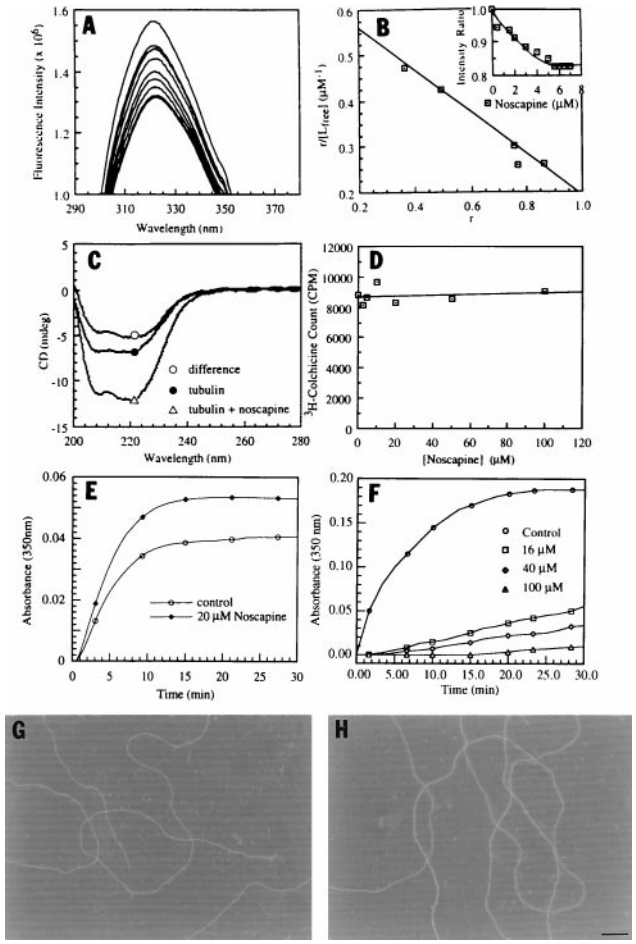

FIG. 7. Noscapine induces conformational change on binding tubulin and alters microtubule assembly. (*A*) Fluorescence quenching of tubulin by noscapine. (*B*) Scatchard plot showing an apparent dissociation constant (K_d) of $1.86 \pm 0.34 \times 10^{-6}$ M and an stoichiometry of 0.95 ± 0.02 noscapine molecule per complex of tubulin subunit. (*Inset*) Saturation of the noscapine-induced quenching in tubulin fluorescence intensity. (*C*) CD spectra of 2.4 μM tubulin in the absence or in the presence of 3.3 μM noscapine in 10 mM sodium phosphate/0.1 mM GTP buffer (pH 7.00) at room temperature. (*D*) [^{3}H]Colchicine binding competition with noscapine. (*E*) Noscapine promotes microtubule assembly in PEM/DMSO solution. (*F*) Noscapine inhibits microtubule assembly in PG/glycerol buffer. (*G* and *H*) Electron microscopy from control and noscapine-treated microtubules. (Bar = 0.15 μm.)

properties of the tubulin–colchicine complex. Consistent with the results with the radioactive colchicine, we did not detect any competition between noscapine and colchicine for binding tubulin (data not shown).

To determine the affect of noscapine upon the assembly of tubulin subunits, we measured changes in turbidity in the absence or presence of noscapine in tubulin at 37°C. Surprisingly, 20 μM noscapine in a PEM/DMSO solution slightly promoted both the rate (i.e., initial slope) and extent of microtubule assembly (Fig. 7*E*). However, in PG/glycerol buffer, noscapine, like colchicine, inhibited microtubule polymerization in a concentration-dependent manner (Fig. 7*F*).

To examine whether the turbidity changes in microtubule assembly assays in the presence of noscapine are due to the aggregate or polymers of aberrant morphology, we used electron microscopy to determine the nature of the polymer in the control and noscapine-treated samples. In PEM/DMSO solution, the samples from noscapine-treated (Fig. 7*H*) and the control (Fig. 7*G*) groups were indistinguishable, in that both contained long polymers. The morphologies of the polymers were also similar in PG/glycerol buffer (data not shown).

DISCUSSION

Our results show that noscapine binds tubulin subunits, alters tubulin assembly, arrests a variety of mammalian cells in mitosis, causes apoptosis in cycling cells, and has potent antitumor activity. Although it has long been argued that drugs that affect microtubule assembly will be effective against tumors through their inhibition of mitosis, our evidence with noscapine supports the view that antitumor activity may arise through initiation of apoptosis in cycling cells.

This may also be true for previously used agents known to cause mitotic arrest. For example, taxol promotes tubulin assembly and inhibits microtubule depolymerization (23). It blocks mitosis, induces extensive formation of microtubule bundles in cells, and induces the formation of multinucleated cells (24, 25). The other agents are colchicine analogs and vinblastine, which arrest cells in mitosis. However, the nanomolar concentrations at which these agents can cause mitotic arrest are well below their ability to depolymerize microtubules (26). It has thus been suggested that these drugs act by a mechanism of kinetic stabilization. The idea is that vinblastine or the colchicine–tubulin complex can cap the kinetically active plus ends of microtubules and hence suppress microtubule dynamics at this end. This idea is very attractive because it can explain the affects of substoichiometric concentrations of these drugs on mitosis (26). However, a more satisfying explanation may lie in the poorly understood relationship between disrupted mitosis and apoptosis. We have not found an appreciable effect of noscapine at the substoichiometric nanomolar concentrations on mitosis *in vivo* or microtubule polymerization *in vitro.* It is clear that noscapine-bound tubulin subunits can assemble into microtubules and that stoichiometric micromolar concentrations are required to elicit these effects.

Although noscapine has chemical moieties that similar to those of colchicine and podophyllotoxin, the [^{3}H]colchicine/noscapine binding competition experiment and the effects of noscapine on the fluorescence time course of colchicine binding to tubulin suggest that noscapine and colchicine probably bind to different sites on tubulin. Superficially, noscapine shares similar chemical groups with colchicine and podophyllotoxin; however, the stereostructure of noscapine, colchicine, and podophyllotoxin differ. Thus, it is possible that noscapine may form other contacts on the surface of tubulin.

Under different buffer condition, noscapine displays apparently opposite behaviors in microtubule assembly. In PEM/DMSO solution, noscapine seems to slightly stimulate the microtubule assembly. In addition, the properties of these microtubules are not different from the native microtubules in that the noscapine-treated microtubules are neither cold-stable nor calcium-resistant, as in the case for taxol-treated microtubules. On the contrary, in PG buffer, noscapine inhibits microtubule assembly. Under electron microscopic examination (Fig. 7 *G* and *H*), noscapine-treated microtubules are not distinguished from the control samples. Currently, we do not know why noscapine–tubulin complexes polymerize so differently from each other under different conditions.

Currently used microtubule drugs are effective antitumor agents, but they produce a variety of side effects (for reviews, see refs. 6 and 27). The wide spectrum of toxicity of these existing drugs is not unanticipated because, besides chromosome segregation during mitosis, microtubules perform a variety of functions in the interphase cells and in postmitotic differentiated cells, such as neurons. Our dose of noscapine in the animal experiments is within the safe range of clinical studies (22). Although at a lower dose (20 mg/kg), noscapine also showed promising results, at a higher dose (120 mg/kg), the antitumor activity was better. The significant *in vivo* antitumor activity coupled with its minimal toxicity is probably derived from the weak interaction between noscapine and tubulin. Noscapine does not bind to tubulin as strongly as colchicine, but its interaction is adequate to arrest mitosis (Figs. 2 and 3). As a consequence, it may be that the mechanism by which noscapine kills cancer cells is a result of this kinetics stabilization of the microtubules and not the action of noscapine on the assembly and disassembly of the polymer. Perhaps it is this relatively unique combination of properties that makes noscapine so special. Collectively, these data argue strongly that noscapine and its analogs may be good chemotherapeutic agents for the treatment or clinical management of some types of human cancers.

We thank Dr. Mats O. Karlsson for generously providing various noscapine-related compounds and discussions; Dr. M.J. Bevan for E.G7-OVA cells; Linda M. Kapp, Carrie Sun, Joel Timberley, and Jessica Mantione for technical assistance; Dr. Guy Benian and Dr. Robert Santoianni for help with histology; and Dr. T. Keane for introducing us to the transitional cell carcinoma model. We also thank Dr. Don Cleveland and Dr. Winfield Sale for carefully reading the manuscript Dr. Don McCormick and Dr. Keith Wilkinson for discussions. We also thank Dr. Thomas D. Pollard (the monitoring editor) and three anonymous reviewers for very good suggestions that improved this article tremendously. This work is partially supported by grants to H.C.J and J.A.K from the National Institutes of Health and grants from the American Cancer Society, the American Heart Association, and the University Research Committee of the Emory University School of Medicine to H.C.J.

1. Hartwell, L. H. & Weinert, T. A. (1989) *Science* **246,** 629–634.
2. Murray, A. W. (1994) *Curr. Opin. Cell Biol.* **6,** 872–876.
3. White, E. (1996) *Genes Dev.* **10,** 1–5.
4. Bose, R., Verheij, M., Haimovitz-Friedman, A., Scotto, K., Fuks, Z. & Kolesnick, R. (1995) *Cell* **82,** 405–414.
5. Epstein, R. J. (1990) *J. Clin. Oncol.* **8,** 2062–2084.
6. Rowinsky, E. K. & Donehower, R. C. (1991) *Pharmacol. Ther.* **52,** 35–84.
7. Empey, D. W., Laitinen, L. A., Young, G. A., Bye, C. E. & Hughes, D. T. D. (1979) *Eur. J. Clin. Pharmacol.* **16,** 393–397.
8. Dahlstrom, B., Mellstrand, T., Lofdahl, C. G. & Johansson, M. (1982) *Eur. J. Clin. Pharmacol.* **22,** 535–539.
9. Karlsson, M. O., Dahlstrom, B., Eckernas, S. A., Johansson, M. & Alm, A. T. (1990) *Eur. J. Clin. Pharmacol.* **39,** 275–279.
10. Karlsson M. O., Dahlstrom, B. & Neil, A. (1988) *Eur. J. Pharmacol.* **145,** 195–203.
11. Mourey, R. J., Dawson, T. M., Barrow, R. K., Enna, A. E. & Snyder, S. H. (1992) *Mol. Pharmacol.* **42,** 619–626.
12. Mitchell, I. D., Carlton, J. B., Chan, M. Y. W., Robinson, A. & Sunderland, J. (1991) *Mutagenesis* **6,** 479–486.
13. Gatehouse, D. G., Stemp, G., Pascoe, S., Wilcox, P., Hawker, J. & Tweats, D. J. (1991) *Mutagenesis* **6,** 279–283.
14. Tsunoda, N. & Yoshimuda, H. (1979) *Xenobiotica* **9,** 181–187.
15. Haikala, V., Sothmann, A. & Marvola, M. (1986) *Eur. J. Clin. Pharmacol.* **31,** 367–369.
16. Moore, M. W., Carbone, F. R. & Bevan, M. J. (1988) *Cell* **54,** 777–785.
17. Darzynkiewicz, Z., Bruno, S., Del Bino, G., Gorczyca, W., Hotz, M. A., Lassota, P. & Traganos, F. (1992) *Cytometry* **13,** 795–808.
18. Walton, M. I., Whysong, D., O'Connor, P. M., Hockenbery, D., Korsmeyer, S. J. & Kohn, K. W. (1993) *Cancer Res.* **53,** 1853–1861.
19. Gorczyca, W., Gong, J. & Darzynkiewicz, Z. (1993) *Cancer Res.* **53,** 1945–1951.
20. Peyrot, V., Leynadier, D., Sarrazin, M., Briand, C., Menendez, M., Laynez, J. & Andreu, J. M. (1992) *Biochemistry* **31,** 11125–11132.
21. O'Brien, E. T., Jacobs, R. S. & Wilson, L. (1983) *Mol. Pharmacol.* **24,** 493–499.
22. Lasagna, L., Owens, A. H., Shnider, B. I. & Gold, G. L. (1961) *Cancer Chemother. Rep.* **15,** 33–34.
23. Schiff, P. B., Fant, J. & Horwitz, S. B. (1979) *Nature (London)* **277,** 665–667.
24. Kalechman, Y., Shani, A., Dovrat, S., Whisnant, J. K., Mettinger, K., Albeck, M. & Sredni, B. (1996) *J. Immunol.* **156,** 1101–1109.
25. Schiff, P. B. & Horwitz, S. B. (1980) *Proc. Natl. Acad. Sci. USA* **77,** 1561–1565.
26. Wilson, L. & Jordan, M. A. (1995) *Chem. Biol.* **2,** 569–573.
27. Kavanagh, J. J & Kudelka, A. P. (1993) *Curr. Opin. Oncol.* **5,** 891–899.